

# Control Strategy for Accurate Reactive Power Sharing in Islanded Microgrids

Xuan Hoa Thi Pham<sup>†</sup> and Toi Thanh Le<sup>\*</sup>

<sup>†,\*</sup>Dept. of Electrical and Electronic Engineering, University of Food Industry, Ho Chi Minh City, Vietnam

## Abstract

This paper presents a control strategy to enhance the accuracy of reactive power sharing between paralleled three-phase inverters in an islanded microgrid. In this study, the mismatch of power sharing when the line impedances have significant differences between inverters connected to a microgrid has been solved, the accuracy of the reactive power sharing in an islanded microgrid is increased, the voltage droop slope is tuned to compensate for the mismatch of voltage drops across the line impedances by using an enhanced droop controller. The proposed method ensures accurate power sharing even if the microgrid has local loads at the output of the inverters. The control model has been simulated by MATLAB/Simulink with two or three inverters connected in parallel. Simulation results demonstrate the accuracy of the implemented control method. Furthermore, in order to validate the theoretical analysis and simulation results, an experimental setup was built in the laboratory. Results obtained from the experimental setup verify the effectiveness of the proposed method.

**Key words:** Droop control, Microgrid control, Parallel inverter, Power sharing, Virtual impedance

## I. INTRODUCTION

Microgrids are attracting a lot of attention since they can alleviate the stress of main transmission systems, reduce feeder losses and improve the quality of power systems. Microgrids consist of multiple parallel-connected distributed generation (DG) units with coordinated control strategies, which are able to operate in both grid-connected and islanded modes. It is important to maintain systematic stabilities and achieve load power sharing among numerous parallel-connected DG units when islanded microgrids are concerned. However, the poor active and reactive power sharing problems due to the influence of the impedance mismatch of DG feeders and the different ratings of DG units are inevitable when a conventional droop control scheme is adopted. The control strategies for islanded microgrid are usually divided into two main types [1], [2]. The first type is made up of communication-based control techniques including concentrated control, master/slave control and distributed control. Although these techniques

can achieve an excellent power sharing, they require communication lines between modules which may increase the cost of systems. Long distance communication lines are easy to disrupt and reduce both system reliability and expandability. The second type is based on the droop control technique, and it is widely used in conventional power systems [2]-[11]. The reason for the popularity of this droop control technique is that it provides a decentralized control capability that does not depend on external communication links. These techniques enable the “plug-and-play” interface and increase the reliability of systems. However, communications can be used in addition to the droop control method in order to enhance the system performance without reducing reliability [12]-[22].

Traditional droop control techniques have some drawbacks in terms of power sharing for the following reasons.

- The line impedances are not available and different from each other, which has a significant effect on power sharing due to different voltage drops. When the impedances of the lines connecting inverters to the common connection point are different, a current imbalance appears since the load sharing error increases [1].
- The heterogeneous line impedance, including the resistor and capacitance, is not suitable for the conventional droop control with pure resistors or pure capacitance

Manuscript received Nov. 7, 2018; accepted Mar. 18, 2019

Recommended for publication by Associate Editor Yun Zhang.

<sup>†</sup>Corresponding Author: hoaptx@hufi.edu.vn

Tel: 989-969-660, University of Food Industry

<sup>\*\*</sup>Dept. of Electr. & Electron. Eng., University of Food Industry, Vietnam

applied for the low voltage distribution [1], [22]. Moreover, with a heterogeneous line impedance, the active and reactive powers interact with each other, which leads to difficulty for the separate control [1].

Although frequency droop techniques can achieve accurate real power sharing, they typically result in poor reactive power sharing due to mismatches in the impedances of the DG unit feeders and the different ratings of the DG units [22]-[24]. Consequently, the problem of reactive power sharing in islanded microgrids has received considerable attention in the literature and many control techniques have been developed to address this issue [24], [25]. In addition, an adaptive voltage droop control was presented in [26] to share the reactive power. The effect of the mismatched feeder impedance is compensated by adaptive droop coefficients and reactive power sharing can be achieved. This method is immune to communication delay. However, nonlinear and unbalanced loads are not considered. An enhanced control strategy was presented in [27] to accurately share reactive power, where the active power disturbance is adopted to identify the error of the reactive power sharing and is eliminated by using a slow integral term. Unfortunately, the signal injection method deteriorates the power quality and affects the systematic stability. To regulate unbalanced power and reactive power, an adaptive inverse control with an enhanced droop control algorithm has been implemented to adjust the weight coefficients of digital filters in real time [28]. However, the reactive power sharing of an islanded MG might be poor if the microgrid has local loads at the output of the DGs. Since a communication delay always exists in hierarchical control, the output correction signals sent to the primary control need a time delay due to the communication lines, which results in damage to microgrid systems. To achieve a better active and reactive power sharing, the communication delay caused by low bandwidth communication lines need to be considered.

It is difficult to share reactive power accurately under a mismatched feeder impedance, nonlinear loads and unbalanced load conditions by the enhanced droop control. As a supplement of the enhanced droop control, methods based on virtual impedance or improved virtual impedance, have been proposed to share the active and reactive powers [29]-[34]. Although inductive virtual impedance can enhance the capacity of the reactive power sharing under mismatched feeder impedance conditions, the virtual impedance reduces the voltage of microgrids.

The problem of the reactive power sharing in islanded microgrids has received a lot of attention in the literature and many control techniques have been developed to address this issue [35]-[37], where a mixed H2/H $\infty$  based on a voltage control loop and a sliding-mode-control (SMC) based on a current loop, is used as a replacement for the conventional proportional-plus-integral-based cascaded control. This

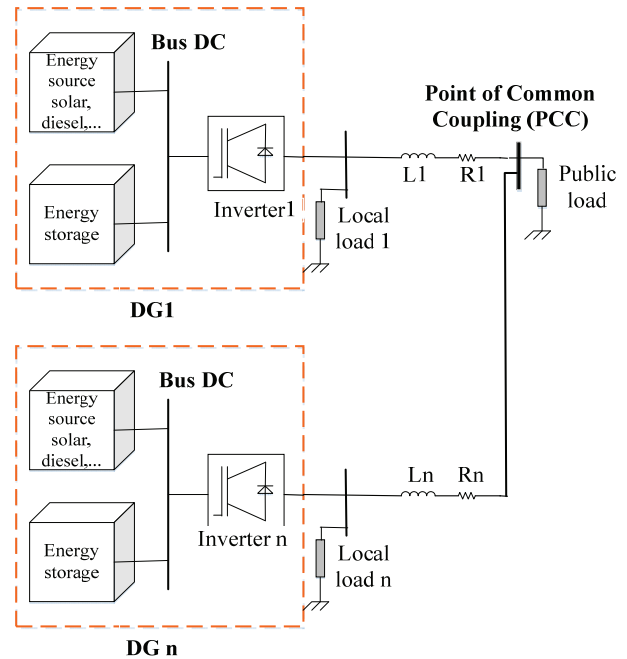


Fig. 1. Block diagram of inverters in an islanded microgrid.

controller can improve the sustainability of the control system if the microgrid has both nonlinear loads and unbalanced loads. However, the mathematical model for SMC controllers is relatively complex, especially when there are local loads.

The focus of this paper is a proposed method for controlling parallel connected inverters in an islanded microgrid to allow for power sharing according to the ratio of the rated power of the inverters under the following conditions.

- There are significant differences in the line parameters from the inverters to the point of common coupling (PCC).
- The microgrid has the local loads connected at the output of the inverters.

## II. ISLANDED MICROGRID CONTROL

### A. The Proposed Control Method

The structure of an islanded microgrid is made up of many inverters connected in parallel. A block diagram of inverters, where each inverter is connected to a common bus at the PCC through the line impedance, is shown in Fig. 1. In addition, the loads of a microgrid are also connected to the common bus. The implemented controller contains two control loops, where the outer loop power control divides the capacity of each inverter, and the inner loop control makes the voltage and current output of the inverters similar to their references.

### B. The Principle of the Proposed Control Method

The principle of the droop control method is explained by considering the equivalent circuit of an inverter connected to an AC bus. The analysis method is based on Thevenin theorem as shown in Fig. 2.

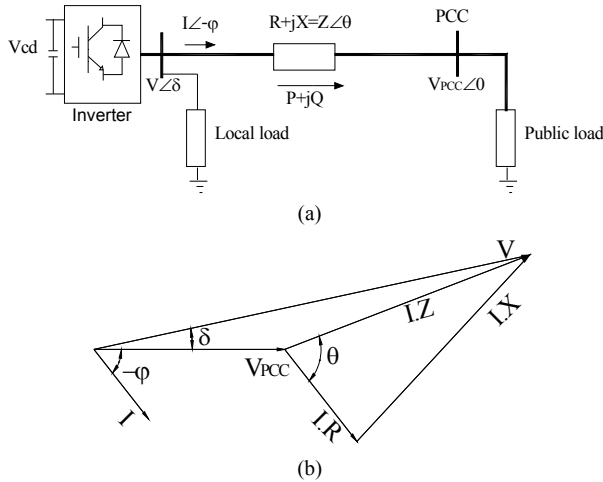


Fig. 2. Diagrams. (a) Equivalent schematic of an inverter connected to loads. (b) Vector diagram of the voltage and current.

The active and reactive powers supplied by the inverter are calculated as follows:

$$P = \frac{V}{R^2 + X^2} [R(V - V_{PCC} \cos \delta) + XV_{PCC} \sin \delta] \quad (1)$$

$$Q = \frac{V}{R^2 + X^2} [-RV_{PCC} \sin \delta + X(V - V_{PCC} \cos \delta)] \quad (2)$$

When the angle  $\delta$  is small and  $X \gg R$ , equations (1) and (2) are rewritten as:

$$\delta \cong \frac{XP}{VV_{PCC}} \quad (3)$$

$$V - V_{PCC} \cong \frac{XQ}{V} \quad (4)$$

From (3) and (4), the basis of well-known frequency and voltage droop regulation through active and reactive powers are calculated by:

$$\omega - \omega_0 = -m_p(P - P_0) \quad (5)$$

$$V - V_0 = -m_q(Q - Q_0) \quad (6)$$

where  $V_0$  and  $\omega_0$  are the nominal amplitude voltage and frequency of the inverter,  $V$  and  $\omega$  are the measured amplitude voltage and frequency of the inverter,  $P$  and  $Q$  are the active power and reactive power output of the inverter,  $P_0$  and  $Q_0$  are the nominal active power of the inverter and the nominal reactive power of the inverter, and  $m_p$  and  $m_q$  are the active and reactive droop coefficients, which are calculated as follows:

$$m_p = \frac{\omega_0 - \omega_{min}}{P_{max} - P_0}; m_q = \frac{V_0 - V_{min}}{Q_{max} - Q_0} \quad (7)$$

The impedance of the lines connecting the inverters to the PCC is significantly different, the load sharing accuracy is difficult to achieve and the voltage adjustment is difficult since it depends on the parameters of the system. From (5) and (6), the following are obtained:

$$m_{q1}Q_1 = m_{q2}Q_2 = \dots = m_{qn}Q_n = \Delta V_{max} \quad (8)$$

$$m_{p1}P_1 = m_{p2}P_2 = \dots = m_{pn}P_n = \Delta \omega_{max} \quad (9)$$

Suppose power sharing is controlled for an islanded microgrid that has two parallel inverters. Then it is possible to obtain the following from equation (6):

$$\begin{cases} V_1 = V_0 - m_{q1}Q_1 \\ V_2 = V_0 - m_{q2}Q_2 \end{cases} \Rightarrow \begin{cases} m_{q1}Q_1 = V_0 - V_1 = \Delta V_1 \\ m_{q2}Q_2 = V_0 - V_2 = \Delta V_2 \end{cases} \quad (10)$$

According to equation (10), it can be seen that as a condition for two inverters to achieve reactive power sharing to the correct ratio, they must satisfy the following constraint:

$$\Delta V_1 = \Delta V_2 \Rightarrow V_1 = V_2 \quad (11)$$

Then:

$$m_{q1}Q_1 = m_{q2}Q_2 \quad (12)$$

Equation (4) can be rewritten as:

$$Q = \frac{V}{X}(V - V_{PCC} \cos \delta) \quad (13)$$

Replacing equation (13) into equation (12) yields:

$$m_{q1} \frac{V_1}{X_1}(V_1 - V_{PCC} \cos \delta_1) = m_{q2} \frac{V_2}{X_2}(V_2 - V_{PCC} \cos \delta_2) \quad (14)$$

From equation (11) and equation (14), the following condition must be met for the two inverters to achieve reactive power sharing to the correct ratio:

$$\begin{cases} \frac{m_{q1}}{X_1} = \frac{m_{q2}}{X_2} \\ \delta_1 = \delta_2 \\ V_1 = V_2 \end{cases} \quad (15)$$

Similar to active power sharing, according to equation (5) it is possible to write:

$$\begin{cases} \omega_1 = \omega_0 - m_{p1}P_1 \\ \omega_2 = \omega_0 - m_{p2}P_2 \end{cases} \Rightarrow \begin{cases} m_{p1}P_1 = \omega_0 - \omega_1 = \Delta \omega_1 \\ m_{p2}P_2 = \omega_0 - \omega_2 = \Delta \omega_2 \end{cases} \quad (16)$$

According to equation (16), it can be seen that as a condition for two inverters to share active power to the correct ratio, they must satisfy the following constraint:

$$\Delta \omega_1 = \Delta \omega_2 \Rightarrow \omega_1 = \omega_2 \quad (17)$$

Then:

$$m_{p1}P_1 = m_{p2}P_2 \quad (18)$$

Equation (3) can be rewritten as:

$$P = \frac{VV_{PCC}}{X} \sin \delta \quad (19)$$

Replace equation (19) into equation (18) yields:

$$m_{p1} \frac{V_1 V_{PCC}}{X_1} \sin \delta_1 = m_{p2} \frac{V_2 V_{PCC}}{X_2} \sin \delta_2 \quad (20)$$

From equation (17) and equation (20), the following condition must be met for two inverters to achieve reactive power sharing to the correct ratio:

$$\begin{cases} \frac{m_{p1}}{x_1} = \frac{m_{p2}}{x_2} \\ \delta_1 = \delta_2 \\ V_1 = V_2 \end{cases} \quad (21)$$

Combined with conditions (15) and (21), there are also conditions to active and reactive power sharing in accordance with the norm ratio for two inverters:

$$\begin{cases} \frac{m_{p1}}{m_{p2}} = \frac{x_1}{x_2} \\ \delta_1 = \delta_2 \\ V_1 = V_2 \\ \frac{m_{q1}}{m_{q2}} = \frac{x_1}{x_2} \end{cases} \quad (22)$$

To satisfy (22), it is necessary to choose droop coefficients that are proportional to the line impedance. If the system is adjusted to meet these requirements, the droop affects the quality of the frequency and voltage.

In this paper, a controller is proposed to ensure accurate power sharing of parallel inverters without adjusting the droop coefficients.

### C. Analyze the Effect of Local Loads on Reactive Power Sharing

Active power sharing based on frequency droop is not affected by local loads. However, local loads affecting reactive power sharing during islanding operation [20]-[34], is showed in Fig. 3.

A number of things can be seen in Fig. 3.

When the microgrid does not have local loads, the slope  $k_{q1,2}$  is obtained as follows:

$$k_{q1,2} = \frac{V_{0,1,2} - V_0}{Q_{0,1,2}} \quad (23)$$

When the microgrid has local loads, the slope  $k_q$  is obtained as follows:

$$k_{q1,2} = \frac{V_{0,1,2} - V_0}{Q_{0,1,2} - Q_{0,local1,2}} \quad (24)$$

Where:

$V_0$ : the nominal amplitude voltage at the PCC.

$V_{0,1,2}$ : the nominal amplitude voltage of the inverters 1, 2.

$Q_{0,1,2}$ : the nominal reactive power of the inverters 1, 2.

$Q_{0,local1,2}$ : the nominal reactive power of the local loads 1, 2.

Different local loads or different inverters leading to reactive power sharing is inaccurate as shown in Fig. 4 and Fig. 5.

According to Fig. 4, when the microgrid has local load 1, the slope  $k_{q1}$  is obtained as follows:

$$k_{q1} = \frac{V_{0,1,2} - V_0}{Q_{0,1,2} - Q_{0,local1}} \quad (25)$$

According to Fig. 4, when the microgrid has local load 2, the slope  $k_{q2}$  is obtained as follows:

$$k_{q2} = \frac{V_{0,1,2} - V_0}{Q_{0,1,2} - Q_{0,local2}} \quad (26)$$

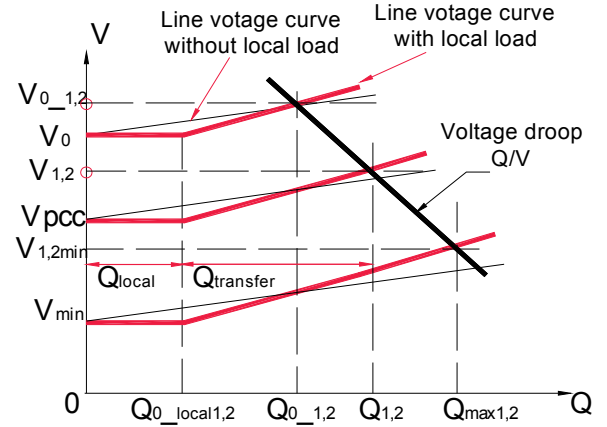


Fig. 3. Reactive power flows of two inverters with local loads and line impedances are the same.

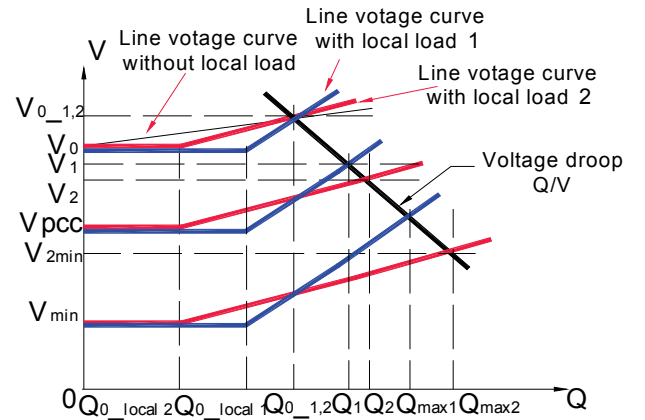


Fig. 4. Reactive power flows of two identical inverters and different local loads.

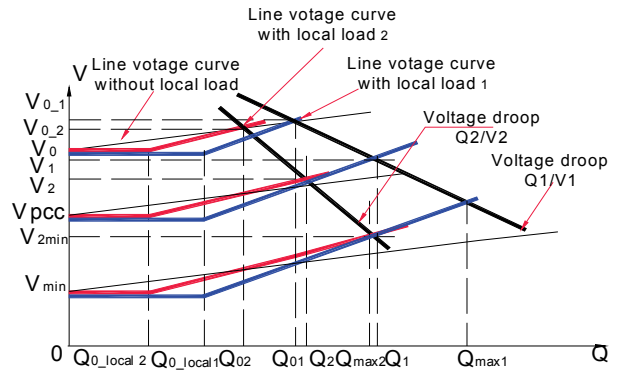


Fig. 5. Reactive power flows of two different inverters and different local loads.

According to Fig. 5, when the microgrid has local load 1, the slope  $k_{q1}$  is obtained as follows:

$$k_{q1} = \frac{V_{0,1} - V_0}{Q_{0,1} - Q_{0,local1}} \quad (27)$$

According to Fig. 5, when the microgrid has local load 2, the slope  $k_{q1}$  is obtained as follows:

$$k_{q2} = \frac{V_{0,2} - V_0}{Q_{0,2} - Q_{0,local2}} \quad (28)$$

Where:

$V_{0,1}$ : the nominal amplitude voltage of inverter 1.

$V_{0,2}$ : the nominal amplitude voltage of inverter 2.

$Q_{0,1}$ : the nominal reactive power of inverter 1.

$Q_{0,2}$ : the nominal reactive power of inverter 2.

$Q_{0,local1}$ : the nominal reactive power of local load 1.

$Q_{0,local2}$ : the nominal reactive power of local load 2.

Figs. 3, 4 and 5 show that when a microgrid has local loads at the output of the inverters, which changes the output voltage of the inverters, the voltage of the local loads is equal to the voltage at the PCC. Therefore, the local loads make an offset in the output voltage of the inverters, which is the cause of the mismatch for reactive power sharing in islanded microgrids.

In the general case, the slope  $k_{qi}$  can write as follows:

$$k_{qi} = \frac{V_i - V_{PCC}}{Q_i} = \frac{\Delta V}{Q_i} \quad (29)$$

$V_i$  is voltage at the output of the inverter.

$V_{PCC}$  is voltage at the PCC.

$Q_i$  is the reactive power at the output of the inverter.

Where:

$$\Delta v = v_i - v_{PCC} = Ri_2 + L \frac{di_2}{dt} \quad (30)$$

Equation (30) can be written as:

$$\Delta V_d = Ri_{2d} + L \frac{di_{2d}}{dt} - \omega Li_{2q} \quad (31)$$

$$\Delta V_q = Ri_{2q} + L \frac{di_{2q}}{dt} + \omega Li_{2d} \quad (32)$$

$i_2$  is the current running through the line impedance.

$R(\Omega)$  is the line resistor, and  $L(H)$  is the line inductance.

#### D. Proposed Droop Controller

A number of things can be seen in Fig. 6.

- If  $V_{pcc} < V_{min}$  (the minimum allowable voltage), the reactive power at the output of the inverters is larger than its maximum value ( $Q_1 > Q_{1max}$  and  $Q_2 > Q_{2max}$ ). This reactive power sharing inaccurately leads to the risk of exceeding the inverter current ratings. Moreover,  $V_{pcc} < V_{min}$ , which is unacceptable to the sensitive loads.
- If  $V_{pcc} > V_{min}$ , the reactive power at the output of inverters is smaller than its maximum value ( $Q_1 < Q_{1max}$  and  $Q_2 < Q_{2max}$ ). In this case, the power sharing is made possible, which ensures the quality of the voltage delivered to loads.
- If  $V_{pcc} = V_0$ , the reactive power at the output of the inverters is equal to its rated value ( $Q_1 = Q_{0,1}$  and  $Q_2 = Q_{0,2}$ ). In this case, the power sharing is made possible, which ensures the quality of the voltage delivered to loads.

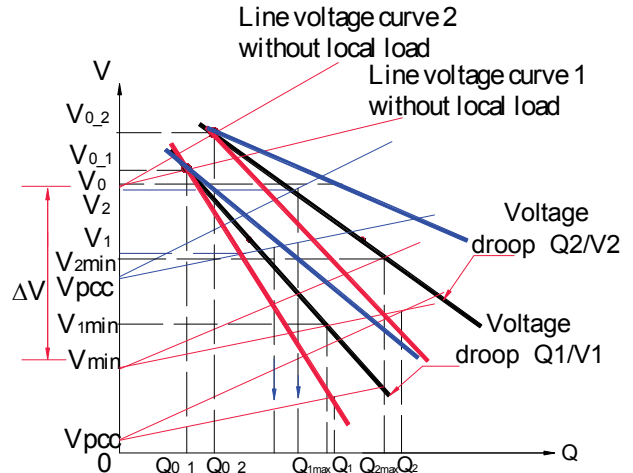


Fig. 6. Reactive power flows of two inverters and line impedances that are different.

On the other hand, as shown in Fig. 6, if the  $k$  slope is not considered, which can lead to one or more of the inverters generating reactive power beyond the maximum limit. In addition, the minimum system voltage (voltage at the PCC) is  $V_{min}$ . As a result, there are risks of operating DG systems beyond the maximum rating and the microgrid voltage dropping below the minimum allowable value. To realize accurate power sharing, the accuracy of reactive power sharing in islanding microgrid operation can be enhanced by incorporating the slope  $k_{qi} = \frac{\Delta V_i}{Q_i}$  and modifying the voltage droop slope (Q/V). This method is shown as follows.

- If  $V_{pcc} = V_0$ , Fig. 6 shows the output voltages of the inverters:  $V_{0,1}, V_{0,2}, \dots, V_{0,n}$ , slope  $k_{qi}$ :

$$k_{qi} = \frac{V_{0,i} - V_0}{Q_{0,i}} \quad (33)$$

Equation (33) can be written as:

$$V_{0,i} = V_0 + k_{qi} \cdot Q_{0,i} \quad (34)$$

- If  $V_{pcc} = V_{min}$ , Fig. 6 shows the output voltages of the inverters:  $V_{1min}, V_{2min}, \dots, V_{nmin}$ , slope  $k_{qi}$ :

$$k_{qi} = \frac{V_{imin} - V_{min}}{Q_{imax}} \quad (35)$$

Equation (35) can be written as:

$$V_{imin} = V_{min} + k_{qi} \cdot Q_{imax} \quad (36)$$

Equations (34) and (36) can be obtained by the voltage droop slope (Q/V):

$$m_{qi} = \frac{V_{0,i} - V_{imin}}{Q_{0,i} - Q_{imax}} \quad (37)$$

The droop control (Q/V) is given by:

$$V_i = V_{0,i} - m_{qi}(Q_{0,i} - Q_i) \quad (38)$$

### E. Proposed Droop Controller when the Microgrid has Local Loads

When the microgrid has local loads, the slope  $k_{qi}$  can be written as follows:

$$k_{qi} = \frac{V_i - V_{PCC}}{Q_i - Q_{local_i}} = \frac{\Delta V}{Q_i - Q_{local_i}} \quad (39)$$

$Q_{local_i}$  is the reactive power of local loads.

- If  $V_{pcc} = V_0$ , slope  $k_{qi}$ :

$$k_{qi} = \frac{V_{0_i} - V_0}{Q_{0_i} - Q_{0_{local_i}}} \quad (40)$$

Equation (40) can be written as:

$$V_{0_i} = V_0 + k_{qi} \cdot (Q_{0_i} - Q_{0_{local_i}}) \quad (41)$$

- If  $V_{pcc} = V_{min}$ , slope  $k_{qi}$ :

$$k_{qi} = \frac{V_{imin} - V_{min}}{Q_{imax} - Q_{0_{local_i}}} \quad (42)$$

Equation (42) can be written as:

$$V_{imin} = V_{min} + k_{qi} \cdot (Q_{imax} - Q_{0_{local_i}}) \quad (43)$$

Equations (41) and (43) can be obtained by the voltage droop slope (Q/V):

$$m_{qi} = \frac{V_{0_i} - V_{imin}}{Q_{0_i} - Q_{imax}} \quad (44)$$

The droop control (Q/V) is given by:

$$V_i = V_{0_i} - m_{qi} (Q_{0_i} - Q_i) \quad (45)$$

The proposed droop controller is formed from equations (39) to (45).

A block diagram of the proposed controller for an islanded microgrid is shown in Fig. 7.

### F. Virtual Impedance

As presented in [20]-[27], based on Fig. 7, the virtual impedance can be established by:

$$v_v = Z_v \cdot i_2 = R_v i_2 + L_v \frac{di_2}{dt} \quad (46)$$

Equation (46) can be written as:

$$v_{dv} = i_{2d} R_v + L_v \frac{di_{2d}}{dt} - i_{2q} \omega L_v \quad (47)$$

$$v_{qv} = i_{2q} R_v + L_v \frac{di_{2q}}{dt} + i_{2d} \omega L_v \quad (48)$$

Equations (47) and (48) can be written as:

$$v_{dv} = i_{2d} R_v - i_{2q} X_v \quad (49)$$

$$v_{qv} = i_{2q} R_v + i_{2d} X_v \quad (50)$$

Where:  $R_v$  is a virtual resistor ( $\Omega$ ), and  $X_v = \omega L_v$  is a virtual reactance ( $\Omega$ ).

### G. Voltage Controller and Current Controller

The voltage controller and the current controller are based on a theorem as shown in Fig. 7.

Where:

$R$  is a line resistor ( $\Omega$ ), and  $L$  is a line inductor (H).

$R_f$  is a line resistor of the filter ( $\Omega$ ), and  $L$  is a line inductor of the filter (H).

Based on Fig. 8, the following equations can be obtained:

$$\begin{cases} i_1 = i_2 + C \frac{dv_c}{dt} + i' \\ v_{inv} = L_f \frac{di_1}{dt} + R_f i_1 + v_c \end{cases} \quad (51)$$

$$\begin{cases} i_{1d} = i_{2d} + C \frac{dv_{cd}}{dt} - \omega C v_{cq} + i'_d \\ i_{1q} = i_{2q} + C \frac{dv_{cq}}{dt} + \omega C v_{cd} + i'_q \end{cases} \quad (52)$$

Equations (51) and (52) can be written as:

$$\begin{cases} i_{1d} = i_{2d} + C \frac{dv_{cd}}{dt} - \omega C v_{cq} + i'_d \\ i_{1q} = i_{2q} + C \frac{dv_{cq}}{dt} + \omega C v_{cd} + i'_q \end{cases} \quad (53)$$

$$\begin{cases} v_{invd} = L_f \frac{di_{1d}}{dt} + R_f i_{1d} - \omega L_f i_{1q} + v_{cd} \\ v_{invq} = L_f \frac{di_{1q}}{dt} + R_f i_{1q} + \omega L_f i_{1d} + v_{cq} \end{cases} \quad (54)$$

$$\begin{cases} v_{invd} = L_f \frac{di_{1d}}{dt} + R_f i_{1d} - \omega L_f i_{1q} + v_{cd} \\ v_{invq} = L_f \frac{di_{1q}}{dt} + R_f i_{1q} + \omega L_f i_{1d} + v_{cq} \end{cases} \quad (55)$$

$$\begin{cases} v_{invd} = L_f \frac{di_{1d}}{dt} + R_f i_{1d} - \omega L_f i_{1q} + v_{cd} \\ v_{invq} = L_f \frac{di_{1q}}{dt} + R_f i_{1q} + \omega L_f i_{1d} + v_{cq} \end{cases} \quad (56)$$

#### 1) Voltage Controller:

Equations (53) and (54) can be written as:

$$\begin{cases} i_{1d} = i_{2d} + C \frac{dv_{cd}}{dt} - \omega C v_{cq} + i'_d = \\ \Delta i_d + i_{2d} - \omega C v_{cq} + i'_d \end{cases} \quad (57)$$

$$\begin{cases} i_{1q} = i_{2q} + C \frac{dv_{cq}}{dt} + \omega C v_{cd} + i'_q = \\ \Delta i_q + i_{2q} + \omega C v_{cd} + i'_q \end{cases} \quad (58)$$

Where:

$$\begin{cases} \Delta i_d = k_{pv}(v_{cd}^* - v_{cd}) + k_{iv} \int (v_{cd}^* - v_{cd}) dt \\ \Delta i_q = k_{pv}(v_{cq}^* - v_{cq}) + k_{iv} \int (v_{cq}^* - v_{cq}) dt \end{cases} \quad (59)$$

$$\begin{cases} \Delta i_d = k_{pv}(v_{cd}^* - v_{cd}) + k_{iv} \int (v_{cd}^* - v_{cd}) dt \\ \Delta i_q = k_{pv}(v_{cq}^* - v_{cq}) + k_{iv} \int (v_{cq}^* - v_{cq}) dt \end{cases} \quad (60)$$

Equations (57) to (60) are for the voltage controller in Fig. 9(a).

#### 2) Current Controller:

Equations (55) and (56) can be written as:

$$\begin{cases} v_{invd} = L_f \frac{di_{1d}}{dt} + R_f i_{1d} - \omega L_f i_{1q} + v_{cd} \\ = \Delta v_d - \omega L_f i_{1q} + v_{cd} \end{cases} \quad (61)$$

$$\begin{cases} v_{invq} = L_f \frac{di_{1q}}{dt} + R_f i_{1q} + \omega L_f i_{1d} + v_{cq} \\ = \Delta v_q + \omega L_f i_{1d} + v_{cq} \end{cases} \quad (62)$$

Where:

$$\begin{cases} \Delta v_d = k_{pi}(i_{1d}^* - i_{1d}) + k_{ii} \int (i_{1d}^* - i_{1d}) dt \\ \Delta v_q = k_{pi}(i_{1q}^* - i_{1q}) + k_{ii} \int (i_{1q}^* - i_{1q}) dt \end{cases} \quad (63)$$

$$\begin{cases} \Delta v_d = k_{pi}(i_{1d}^* - i_{1d}) + k_{ii} \int (i_{1d}^* - i_{1d}) dt \\ \Delta v_q = k_{pi}(i_{1q}^* - i_{1q}) + k_{ii} \int (i_{1q}^* - i_{1q}) dt \end{cases} \quad (64)$$

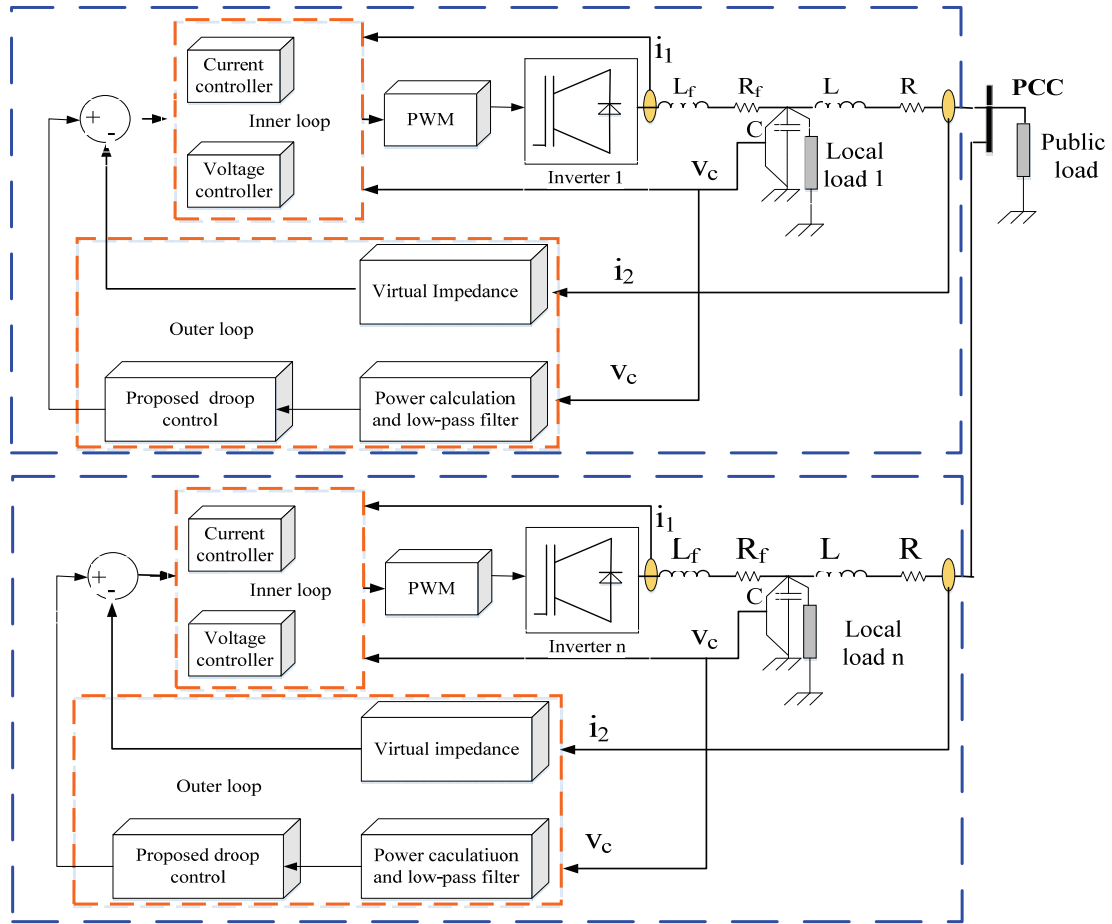


Fig. 7. Block diagram of the proposed controller for an islanded microgrid.

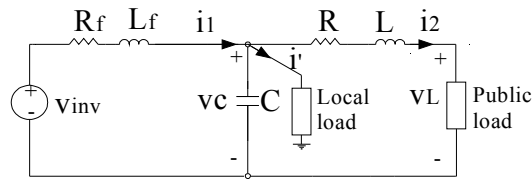


Fig. 8. Equivalent schematic of inverters connected to a load.

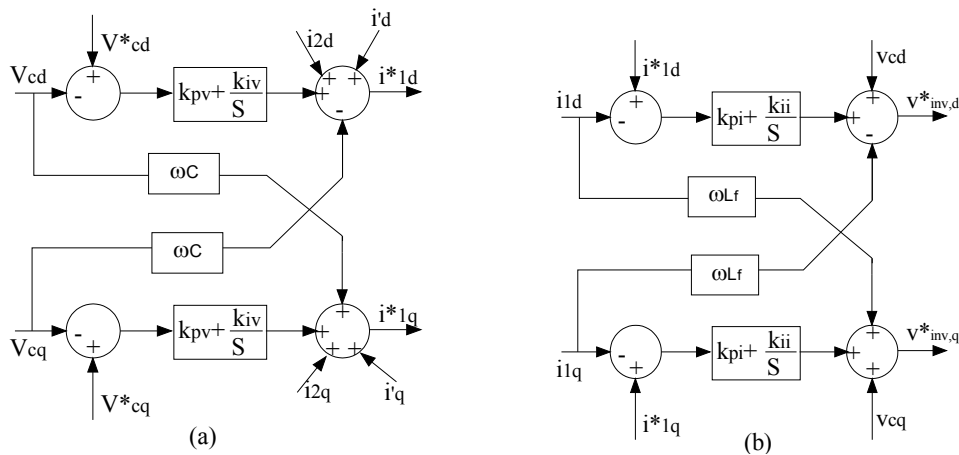


Fig. 9. Schematics. (a) Voltage controller. (b) Current controller.

TABLE I  
PARAMETERS FOR THE CONTROLLERS

Parameters	Values	Parameters	Values
Filter resistance $R_f(\Omega)$	0.2	Rate voltage $V_{AC,p}$ (V)	310
Filter capacitance $C$ ( $\mu\text{F}$ )	50	Droop coefficient $m_q$ (V/Var)	$1.7\text{e-}3$
Switching frequency $f_0$ (kHz)	5	Droop coefficient $m_p$ (rad/s /W)	$1\text{e-}4$
Rate frequency $f_0$ (Hz)	50	Line impedance 1	$0.8\Omega$ ; $0.6\text{mH}$
Rate power (kVA)	4	Line impedance 2	$0.6\Omega$ ; $0.4\text{mH}$
		Virtual impedance 1	$2.4\Omega$ ; $1.8\text{mH}$
		Virtual impedance 2	$1.8\Omega$ ; $1.2\text{mH}$

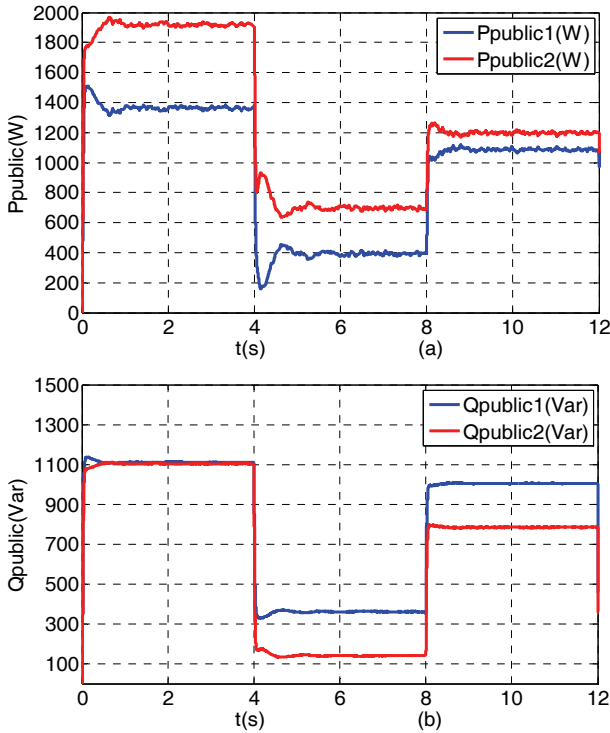


Fig. 10. Power sharing of public loads. (a) Real power. (b) Reactive power.

Equations (61) to (64) are for the current controller in Fig. 9(b).

### III. SIMULATION RESULTS AND DISCUSSION

A microgrid with two or three parallel inverters, as shown in Fig. 1, is simulated by MATLAB/Simulink. All of the simulation parameters of the system are given in Table I.

#### A. Simulation for the Power Sharing of Two Identical Inverters, where the Line Impedances are Different, and the Local Loads and Public Loads are Changed

Simulation results for this case including the real power output, reactive power output, current output and load voltage are shown in Fig. 10.

Fig. 10 shows that the proposed controller achieves good power sharing of public loads when the power of schematic

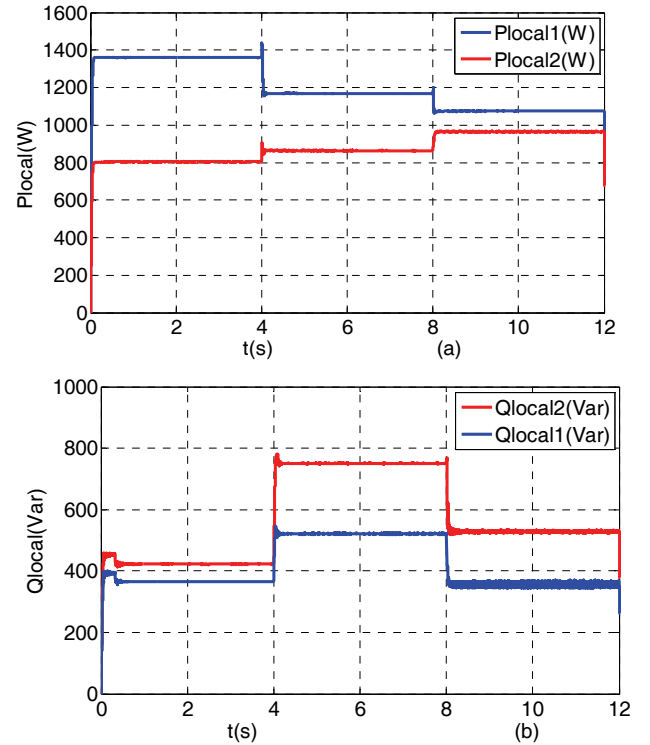


Fig. 11. Power sharing of local loads. (a) Real power. (b) Reactive power.

loads are changed.

Fig. 11 shows that the proposed controller achieves good power sharing of local loads when the power of schematic loads are changed.

Fig. 12 shows that the proposed controller achieves good power sharing of total loads when the power of the loads are changed.

Total output power of each inverter during the period from 0s to 4s:

$$P = 0,5(P_{local1} + P_{local2} + P_{public}) \\ = 0,5(1355 + 800 + 3290) = 2722W$$

$$Q = 0,5(Q_{local1} + Q_{local2} + Q_{public}) \\ = 0,5(350 + 410 + 2200) = 1480Var$$

Total output power of each inverter during the period from 4s to 8s:



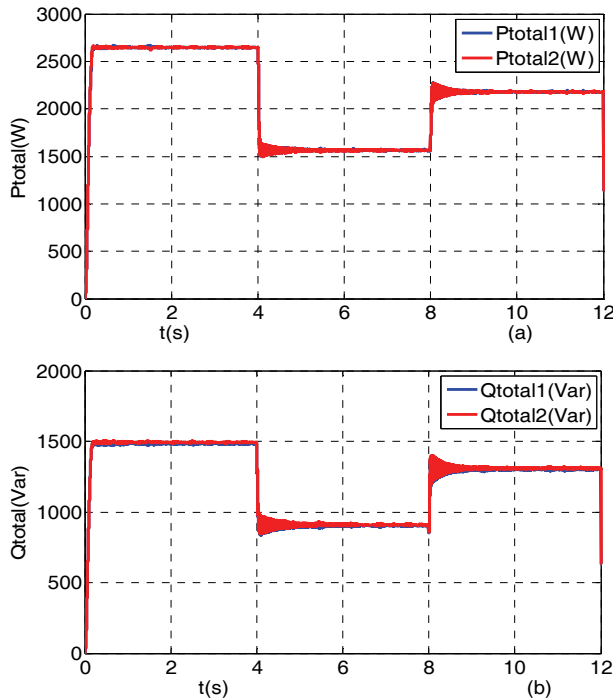


Fig. 12. Power sharing of total loads. (a) Real power. (b) Reactive power.

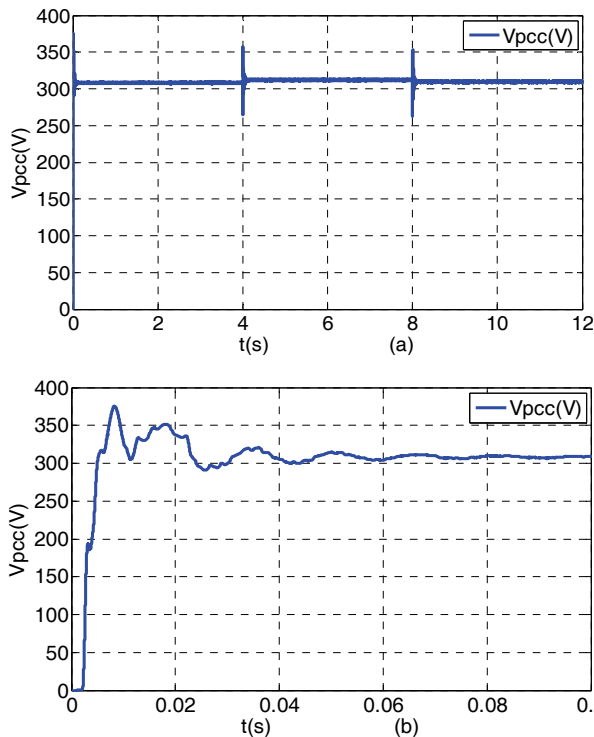


Fig. 13. Voltage at the PCC.

$$P = 0,5(P_{local1} + P_{local2} + P_{public})$$

$$= 0,5(1180 + 880 + 1100) = 1580W$$

$$Q = 0,5(Q_{local1} + Q_{local2} + Q_{public})$$

$$= 0,5(520 + 750 + 470) = 870Var$$

Total output power of each inverter during the period from 8s to 12s:

$$P = 0,5(P_{local1} + P_{local2} + P_{public})$$

$$= 0,5(1090 + 980 + 2280) = 2175W$$

$$Q = 0,5(Q_{local1} + Q_{local2} + Q_{public}) = 0,5(330 + 510 + 1780)$$

$$= 1310Var$$

Fig. 13 shows the voltage quality at the PCC. The voltage quality is always guaranteed by the proposed controller.

### B. Simulation for the Power Sharing of Three Identical Inverters, where the Line Impedances are Different, and the Local Loads and Public Loads are Changed

Fig. 14 shows that the proposed control method provides good power sharing. Figs. 14 accurately shows real and reactive power with a 1:1:1 ratio.

Total output power of each inverter during the period from 0s to 4s:

$$P = \frac{1}{3}(P_{local1} + P_{local2} + P_{local3} + P_{public})$$

$$= \frac{1}{3}(700 + 1300 + 1300 + 4000)$$

$$= 2433W$$

$$Q = \frac{1}{3}(Q_{local1} + Q_{local2} + Q_{local3} + Q_{public})$$

$$= \frac{1}{3}(410 + 340 + 250 + 3200) = 1400Var$$

Total output power of each inverter during the period from 4s to 8s:

$$P = \frac{1}{3}(P_{local1} + P_{local2} + P_{local3} + P_{public})$$

$$= \frac{1}{3}(550 + 850 + 850 + 750) = 1000W$$

$$Q = \frac{1}{3}(Q_{local1} + Q_{local2} + Q_{local3} + Q_{public})$$

$$= \frac{1}{3}(450 + 700 + 550 + 550) = 750Var$$

Total output power of each inverter during the period from 8s to 12s:

$$P = \frac{1}{3}(P_{local1} + P_{local2} + P_{local3} + P_{public})$$

$$= \frac{1}{3}(1000 + 850 + 990 + 2350) = 1700W$$

$$Q = \frac{1}{3}(Q_{local1} + Q_{local2} + Q_{local3} + Q_{public})$$

$$= \frac{1}{3}(550 + 270 + 320 + 2250) = 1230Var$$

## IV. HARDWARE IMPLEMENTATION USING A DSP

In this paper, a practical model has been developed for testing the proposed method. The developed hardware model consists of three 3-phase inverters, Semikron drivers, LEM HX 20P and LV-25P, which are used as voltage and current

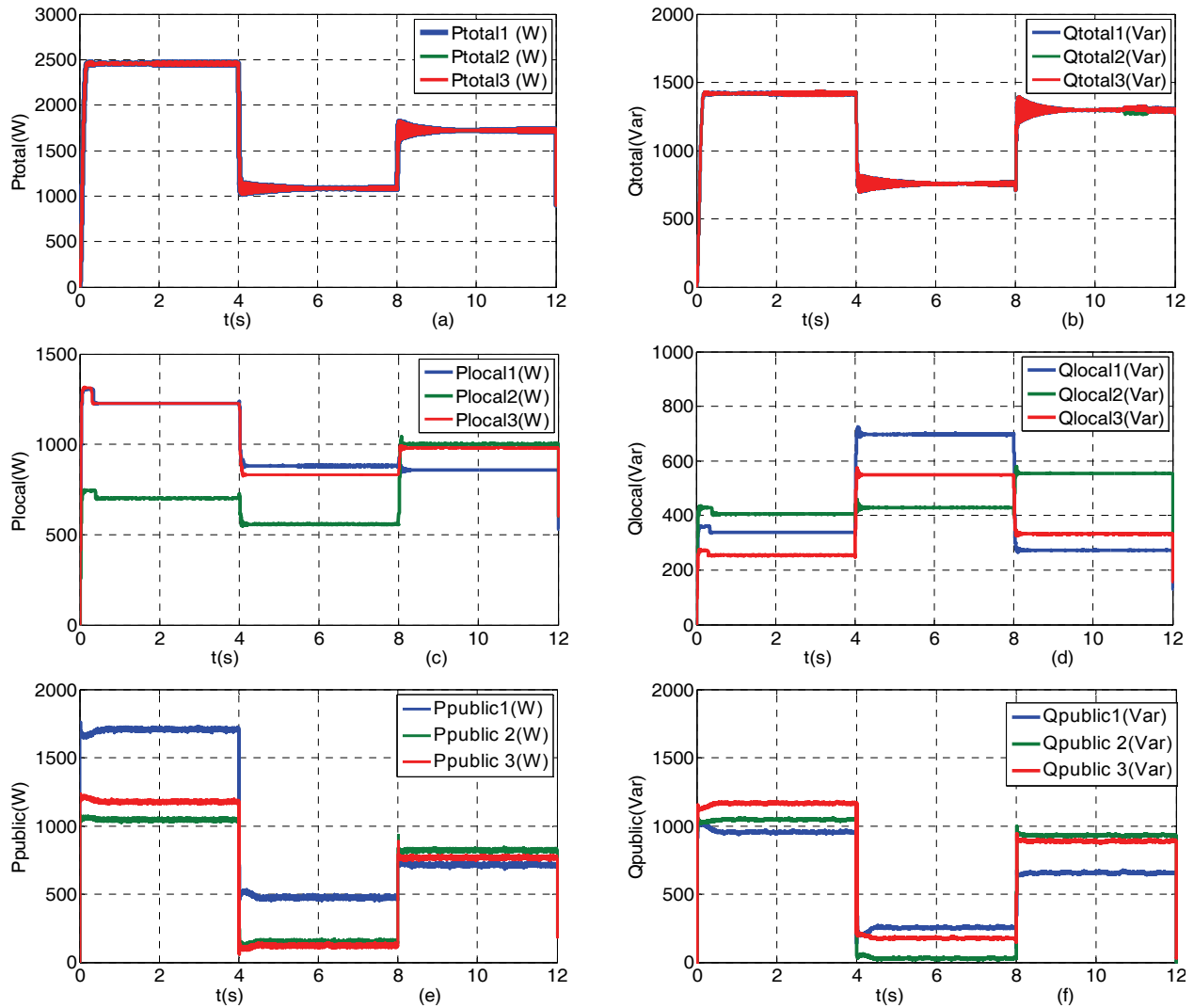


Fig. 14. Power sharing of the total load, local loads and public loads.

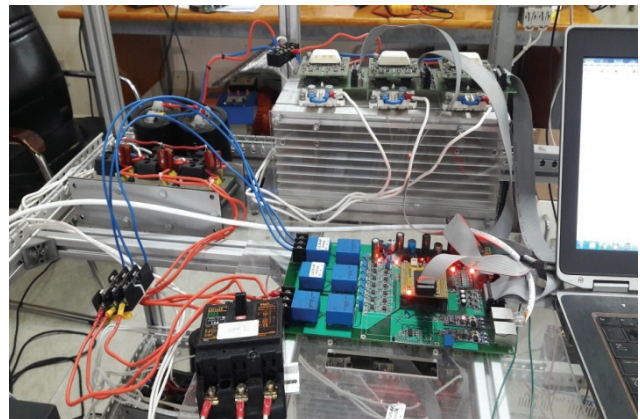


Fig. 15. Hardware setup for the experiment.

sensors, as shown in Fig. 15. The proposed control method has been implemented on a TMS320F28335 DSP controller and the results obtained from the experiment have been captured by a Tektronix TDS2014B oscilloscope and a Fluke 345 PQ

clamp meter. The experiment has been carried out on three test cases with different ratios for the real and reactive powers. The results obtained from the experiment verify the advantages of the proposed control method through case studies.

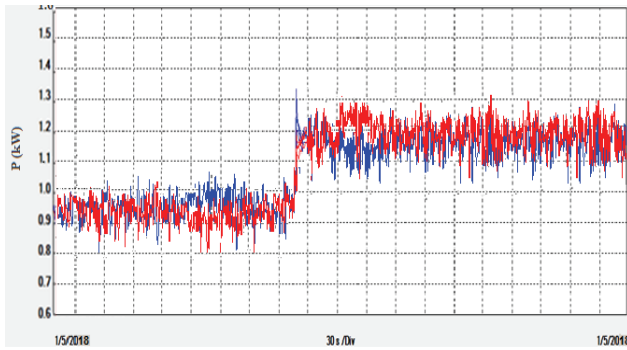


Fig. 16. Real power sharing.

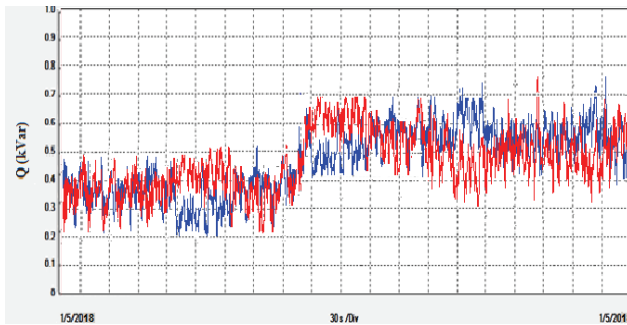


Fig. 17. Reactive power sharing.

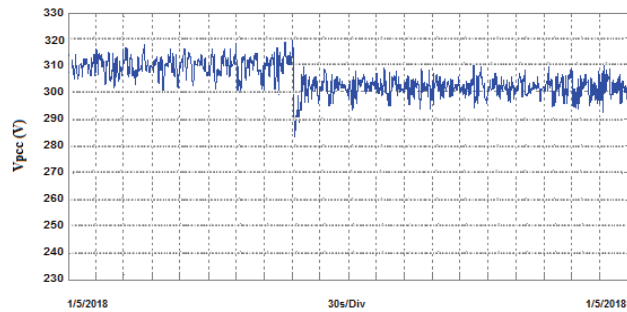


Fig. 18. Voltage at the PCC.

*A. Case Study 1:  $P_1:P_2 = 1:1$ ,  $Q_1:Q_2 = 1:1$ , the Line Impedances are Difference and the Load Changes*

For this case, the ratio of the active and reactive power is 1:1 for two inverters with a load fixed at a pre-determined value. In addition, the line impedances are different. The measured power outputs for the two inverters are shown in Fig. 16 and Fig. 17. The loads are changed from 950 W to 1160W and from 350Var to 550Var. The power sharing errors in this case are very small.

Fig. 18 shows the voltage quality at the PCC. The voltage quality is always guaranteed with the proposed controller.

*B. Case Study 2:  $P_1:P_2:P_3 = 1:1:1$ ,  $Q_1:Q_2:Q_3 = 1:1:1$ , the Line Impedances are Difference and the Load Changes*

Fig. 19 and Fig. 20 show the active and reactive powers of the three inverters in case of load changes. It can be seen that the ratio of the active and reactive powers is still kept at 1:1:1

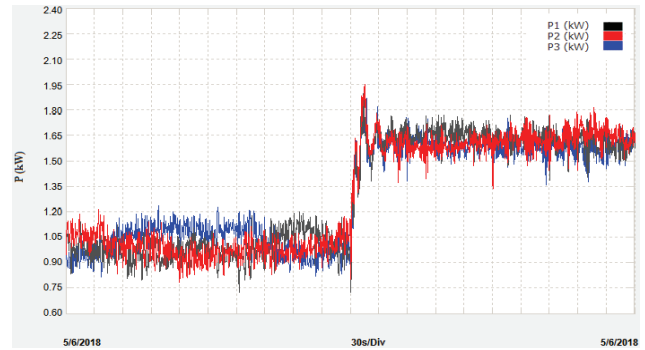


Fig. 19. Real power sharing.

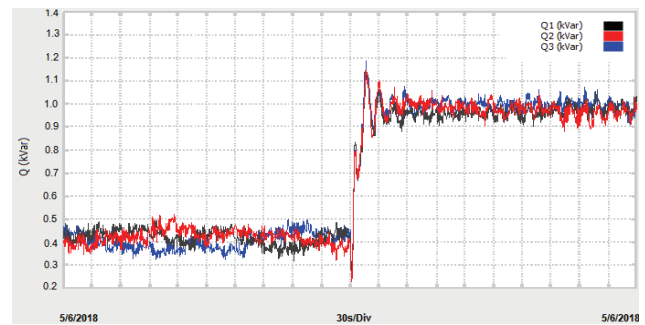


Fig. 20. Reactive power sharing.

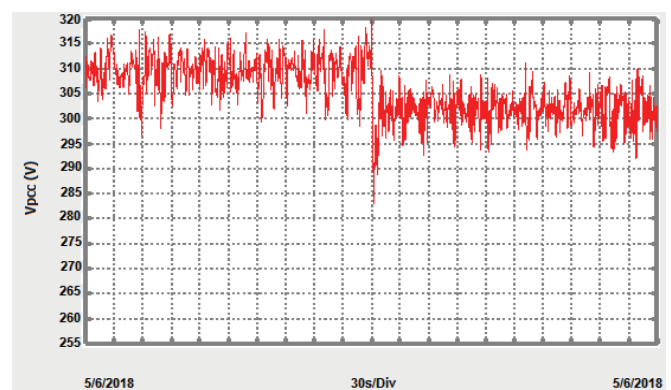


Fig. 21. Voltage at the PCC.

when the load increases and decreases. The loads are changed from 1000 W to 1570W and from 400Var to 970Var. The power sharing errors in this case are very small.

Fig. 21 shows the voltage quality at the PCC. The voltage quality is always guaranteed with the proposed controller.

*C. Case Study 3:  $P_1:P_2:P_3 = 4:2:1$ ,  $Q_1:Q_2:Q_3 = 4:2:1$ , the Line Impedances are Difference and the Load Changes*

This case corresponds to the ratio of the active and reactive powers being 4:2:1, and load changes steps within pre-determined limits. The measured active power outputs for three inverters are shown in Fig. 22, 23 and 24. The obtained active power outputs for the three inverters increase within the limits as  $P_1=2000W$ ,  $P_2=1000W$  and  $P_3=500W$ ; and  $Q_1=800Var$ ,  $Q_2=400Var$  and  $Q_3=200Var$ . These results

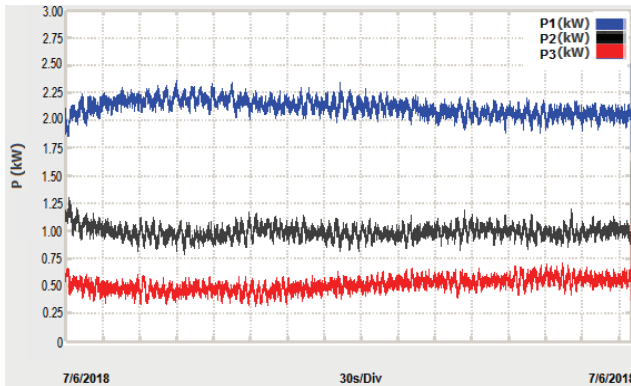


Fig. 22. Real power sharing.

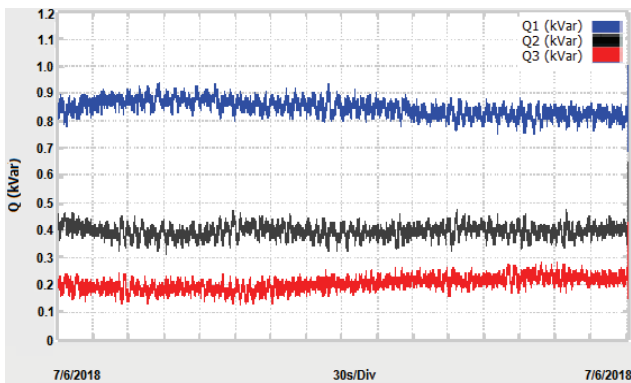


Fig. 23. Reactive power sharing.

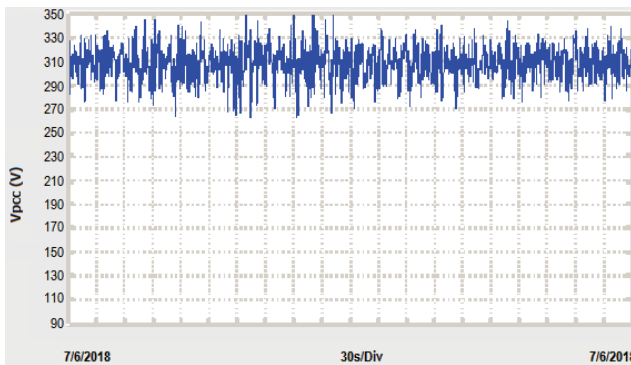


Fig. 24. Voltage at the PCC.

demonstrate the response capability of the system based on the new control strategy when the load continuously changes online with a constant ratio. The active power sharing errors in this case are very small.

Fig. 24 shows the voltage quality at the PCC. The voltage quality is always guaranteed with the proposed controller.

## V. CONCLUSION

This paper has proposed a new method to achieve an accurate load sharing ratio between paralleled inverters in islanded microgrids. In this study, the voltage droop slope is tuned to compensate for mismatch in the voltage drops across

the line impedances by using an improved droop controller. This method ensures accurate power sharing even if a microgrid has local loads. In addition, the accuracy of the power sharing based on the proposed method does not use communication. MATLAB/Simulink simulation results and hardware experiments have demonstrated the superiority of the proposed strategy in any case with any ratio.

## REFERENCES

- [1] H. Han, X. Hou, J. Yang, J. Wu, M. Su, and J. M. Guerrero, "Review of power sharing control strategies for islanding operation of AC microgrids," *IEEE Trans. Smart Grid*, Vol. 7, No. 1, pp. 200-216, Jan. 2016.
- [2] J. Rocabert, A. Luna, F. Blaabjerg, and P. Rodriguez, "Control of power converters in AC microgrids," *IEEE Trans. Power Electron.*, Vol. 27, No. 11, pp. 4734-4739 Nov. 2012.
- [3] Q.-C. Zhong, "Robust droop controller for accurate proportional load sharing among inverters operated in parallel," *IEEE Trans. Power Electron.*, Vol. 60, No. 4, pp. 1281-1291, Apr. 2013.
- [4] Md. A. Hossain, H. R. Pota, W. Issa, and Md. J. Hossain, "Overview of AC microgrid controls with inverter-interfaced generations," *Energies*, Vol. 10, No. 9, Aug. 2017.
- [5] S. V. Iyer, M. N. Belur, and M. C. Chandorkar, "A generalized computational method to determine stability of a multi-inverter microgrid," *IEEE Trans. Power Electron.*, Vol. 25, No. 9, pp. 2420-2432, Sep. 2010.
- [6] J. Justo, F. Mwasilu, and J. Lee, "AC microgrids versus DC microgrids with distributed energy resources: A review," *Renew. Sustain. Energy Rev.*, Vol. 24, pp. 387-405, 2013.
- [7] J. Hu, J. Zhu, D. G. Dorrell, and J. M. Guerrero, "Virtual flux droop method - A new control strategy of inverters in microgrids," *IEEE Trans. Power Electron.*, Vol. 29, No. 9, pp. 4704-4711, Sep. 2014.
- [8] L. Y. Lu and C. C. Chu, "Consensus-based droop control synthesis for multiple DICs in isolated micro-grids," *IEEE Trans. Power Syst.*, Vol. 30, No. 5, pp. 2243-2256, Sep. 2015.
- [9] J. He and Y. W. Li, "An enhanced microgrid load demand sharing strategy," *IEEE Trans. Power Electron.*, Vol. 27, No. 9, pp. 3984-3995, Sep. 2012.
- [10] H. Mahmood, D. Michaelson, and J. Jiang, "Accurate reactive power sharing in an islanded microgrid using adaptive virtual impedances," *IEEE Trans. Power Electron.*, Vol. 30, No. 3, pp. 1605-1618 Mar. 2015.
- [11] J. M. Guerrero, M. Chandorkar, T.-L. Lee, and P. C. Loh, "Advanced control architecture for intelligent microgrids - Part I: Decentralized and hierarchical control," *IEEE Trans. Power Electron.*, Vol. 60, No. 4, pp. 1254-1262 Apr. 2013.
- [12] J. M. Guerrero, J. C. Vasquez, J. Matas, L. G. de Vicuna, and M. Castilla, "Hierarchical control of droop-controlled ac and dc microgrids - A general approach towards standardization," *IEEE Trans. Ind. Electron.*, Vol. 58, No. 1, pp. 158-172, Jan. 2011.
- [13] J. C. Vasquez, J. M. Guerrero, M. Savaghebi, J. Eloy-

- Garcia, and R. Teodorescu, "Modeling, analysis, and design of stationary-reference frame droop-controlled parallel three-phase voltage source inverters," *IEEE Trans. Ind. Electron.*, Vol. 60, No. 4, pp. 1271-1280, Apr. 2013.
- [14] M. Savaghebi, A. Jalilian, J. C. Vasquez, and J. M. Guerrero, "Secondary control scheme for voltage unbalanced compensation in an islanded droop controlled microgrid," *IEEE Trans. Smart Grid*, Vol. 3, No. 2, pp. 797-807, May 2012.
- [15] M. A. Abusara, J. M. Guerrero, and S. M. Sharkh, "Line-interactive ups for microgrids," *IEEE Trans. Ind. Electron.*, Vol. 61, No. 3, pp. 1292-1300, Mar. 2014.
- [16] H. Mahmood, D. Michaelson, and J. Jiang, "Accurate reactive power sharing in an islanded microgrid using adaptive virtual impedances," *IEEE Trans. Power Electron.*, Vol. 30, No. 3, pp. 1605-1617, Mar. 2014.
- [17] J. He, Y. W. Li, J. M. Guerrero, J. C. Vasquez, and F. Blaabjerg, "An islanded microgrid reactive power sharing scheme enhanced by programmed virtual impedances," in *Proc. IEEE Int. Symp. Power Electron. Distrib. Gener. Syst.*, pp. 229-235, 2012.
- [18] J. He, Y. W. Li, J. M. Guerrero, F. Blaabjerg, and J. C. Vasquez, "An islanding microgrid power sharing approach using enhanced virtual impedance control scheme," *IEEE Trans. Power Electron.*, Vol. 28, No. 11, pp. 5272-5282, Nov. 2013.
- [19] S. S. Balasreedharan and S. Thangavel, "An adaptive fault identification scheme for DC Microgrid using event based classification," *International Conference on Advanced Computing and Communication Systems*, pp. 22-23, 2016.
- [20] G. Venkataramanaiah and V. Prasad, "A wireless communication system for data transfer within future micro grids," *Int. J. Mag. Eng.*, Vol. 3, No. 11, pp. 978-985, Nov. 2016.
- [21] M. Farhadi and O. A. Mohammed, "A new protection scheme for multi-bus DC power systems using an event classification approach," *IEEE Trans. Ind. Appl.*, Vol. 52, No. 4, pp. 2834-2842, Jul. 2016.
- [22] M. Ashabani, Y. A.-R. I. Mohamed, M. Mirsalim, and M. Aghashabani, "Multivariable droop control of synchronous current converters in weak grids/microgrids with decoupled dq-axes currents," *IEEE Trans. Smart grid*, Vol. 6, No. 4, pp. 1610-1620, Jul. 2015.
- [23] Mr. Prakash D. Chavan, and R. J. Devi, "Survey of communication system for DG's and microgrid in electrical power grid," *Int. Res. J. Eng. Tech.*, Vol. 3, No. 7, pp. 1155-1164, Jul. 2016.
- [24] B. Moran, "Microgrid load management and control strategies," *IEEE Transmission and Distribution Conference and Exposition*, 2016.
- [25] J.-H. Kim, Y.-S. Lee, H.-J. Kim, and B.-M. Han, "A new reactive-power sharing scheme for two inverter-based distributed generations with unequal line impedances in islanded microgrids," *Energies*, pp. 1-20, Nov. 2017.
- [26] H. Mahmood, D. Michaelson, and J. Jiang, "Reactive power sharing in islanded microgrids using adaptive voltage droop control," *IEEE Trans. Smart Grid.*, Vol. 6, No. 6, pp. 3052-3060, Nov. 2015.
- [27] J. W. He and Y. W. Li, "An enhanced microgrid load demand sharing strategy," *IEEE Trans. Power Electron.*, Vol. 27, No. 9, pp. 3984-3995, Sep. 2012.
- [28] P. Li, X. B. Wang, W. J. Lee, and D. Xu, "Dynamic power conditioning method of microgrid via adaptive inverse control," *IEEE Trans. Power Del.*, Vol. 30, No. 2, pp. 906-913, Apr. 2015.
- [29] K. D. Brabandere, B. Bolsens, J. V. D. Keybus, A. Woyte, J. Driesen, and R. Belmans, "A voltage and frequency droop control method for parallel inverters," *IEEE Trans. Power Electron.*, Vol. 22, No. 4, pp. 1107-1115, Jul. 2007.
- [30] M. Q. Mao, Z. Dong, Y. Ding, and L. C. Chang, "A unified controller for a microgrid based on adaptive virtual impedance and conductance," in *Proc. IEEE Energy Conversion Congress and Exposition (ECCE)*, pp. 695-701, 2014.
- [31] Y. J. Gu, W. H. Li, and X. N. He, "Frequency-coordinating virtual impedance for autonomous power management of DC microgrid," *IEEE Trans. Power Electron.*, Vol. 30, No. 4, pp. 2328-2337, Apr. 2015.
- [32] P. Sreekumar and V. Khadkikar, "A new virtual harmonic impedance scheme for harmonic power sharing in an islanded microgrid," *IEEE Trans. Power Del.*, Vol. 31, No. 3, pp. 936-945, Jun. 2015.
- [33] W. Yao, M. Chen, J. Matas, J. M. Guerrero, and Z. M. Qian, "Design and analysis of the droop control method for parallel inverters considering the impact of the complex impedance on the power sharing," *IEEE Trans. Ind. Electron.*, Vol. 58, No. 2, pp. 576-588, Feb. 2011.
- [34] J. M. Guerrero, M. Chandorkar, T. Lee, and P. C. Loh, "Advanced control architectures for intelligent microgrids-part I: Decentralized and hierarchical control," *IEEE Trans. Ind. Electron.*, Vol. 60, No. 4, pp. 1254-1262, Apr. 2013.
- [35] Z. Li, C. Zang, P. Zeng, H. Yu, and S. Li, "Fully distributed hierarchical control of parallel grid-supporting inverters in islanded AC microgrids," *IEEE Trans. Ind. Informat.*, Vol. 14, No. 2, pp. 679-690, Feb. 2018.
- [36] Z. Li, C. Zang, P. Zeng, H. Yu, H. Li, and S. Li, "Analysis of multi-agent-based adaptive droop-controlled AC microgrids with PSCAD: Modeling and simulation," *J. Power Electron.*, Vol. 15, No. 2, pp. 455-468, Mar. 2015.
- [37] Z. Li, C. Zang, and J. Bian, "Control of a grid-forming inverter based on sliding mode and mixed H2/H $\infty$  control," *IEEE Trans. Ind. Electron.*, Vol. 64, No. 5, pp. 3862-3872, May 2017.



**Xuan Hoa Thi Pham** received her M.S. degree from the University of Technology, Ho Chi Minh City, Vietnam, in 2006; and her Ph.D. degree from the University of Technology, Ho Chi Minh City, Vietnam, in 2018. She has been a Lecturer of Electrical and Electronic Engineering at the University of Food Industry, Ho Chi Minh City, Vietnam, since 2002. Her current research interests include renewable energy interfaces, microgrids and power quality.



**Toi Thanh Le** was born in Tay Ninh, Vietnam, in 1977. He received his M.S. degree in Electronics Engineering from the Ho Chi Minh City University of Technology, Ho Chi Minh City, Vietnam, in 2006. He is presently working as a Lecturer in Faculty of Electrical and Electronics Engineering. His current research interests include power electronics, renewable energy and asynchronous design.